1

2   DR. BRANDON HEDRICK (Orcid ID : 0000-0003-4446-3405)

3

4

6

7

8   Variability and asymmetry in the shape of the spiny dogfish vagina revealed by 2D and 3D

9   geometric morphometrics

10

11   Brandon P. Hedrick*[+1,2], Patricia Antalek-Schrag[+3], Andrew J. Conith[4], Lisa J. Natanson[5],

12   Patricia L. R. Brennan[3]

13

14   [1]Department of Earth Sciences, University of Oxford, Oxford OX1 3AN UK

15   [2]Department of Organismic and Evolutionary Biology, Harvard University, Cambridge MA 02138 USA

16   [3]Department of Biological Sciences, Mount Holyoke College, South Hadley MA 01075 USA

17   [4]Department of Biology, University of Massachusetts Amherst, Amherst MA 01003 USA

18   [5] Northeast Fisheries Science Center, National Marine Fisheries Service, NOAA, Narragansett, RI 02882 USA

19

20   [+]indicates equal work

21   *corresponding author: bphedrick1@gmail.com

22

23

24   Short title: Spiny dogfish vagina variability and asymmetry

25

28

29   **Abstract:**

30   Genital structures are among the most variable in nature and have been suggested to

31 evolve at exceptionally high rates. However, the vast majority of research on genital morphology

32 has been done on male genitalia. We present one of the few studies of female genital shape using

33 geometric morphometrics, and the first of such studies to employ 3D geometric morphometrics,

34 using the spiny dogfish shark, a taxon for which reproductive biology is well-studied. In a

35 sample of 21 adult females, we found no correlation between body size and reproductive and

36 non-reproductive trait size, and therefore no general allometric patterns. Further, we found

37 limited evidence for different 2D and 3D vaginal shapes in visibly pregnant and not visibly

38 pregnant sharks, but trends were more obvious in 3D than 2D. We found high congruence

39 between data derived using 2D geometric morphometrics with that derived from 3D methods.

40 We also found exceptionally high asymmetry in the vagina, again more apparent in 3D than in

41 2D. Visibly pregnant sharks had especially high directional asymmetry (>48% of total variation)

42 likely as a result of an asymmetric distribution of pups in the shark's paired oviducts. Therefore,

43 this asymmetry was functional rather than developmental and presents an important

44 consideration when studying vaginal shape. The lack of significant association between

45 pregnancy and vaginal shape in a species with an extremely long pregnancy suggests that vaginal

46 shape differences may be under additional selective forces such as sexual antagonism during

47 copulation. A combination of 3D geometric morphometric methods along with assessments of

48 asymmetry sheds further light on the growing appreciation that female genitalia is highly

49 variable in shape and may play a substantial role in sexual selection.

50 **Introduction**

51   Genitalia are among the most variable morphological structures in nature (Eberhard

52 1985). Both natural and sexual selection can influence variation in genitalia, but sexual selection

53 is generally accepted as the most common selective force responsible for genital variation

54 (Eberhard, 1985; Hosken & Stockley, 2004; Simmons 2014; Brennan & Prum, 2015). Sexual

55 selection pressures refer to the selective forces that influence the ability of individuals to procure

56 mates including intrasexual competition, intersexual choice, and sexual conflict (Hosken &

57 Stockley, 2004). Natural selection can affect genital variation through mechanisms related to

58 speciation, antipredator protection, mechanical ability to copulate, and oviposition/parturition

59 (Hosken & Stockley, 2004; Simmons 2014; Brennan & Prum 2015; Brennan 2016).

60   Male genital shapes are known to be extremely diverse, especially in insects (Eberhard,

61   1985), but also in vertebrates (Brennan *et al.*, 2008, Brennan & Prum, 2015) and until recently,

62   the highly diverse shapes of male genitals were considered to be the dominant driver behind both

63   male and female genital evolution (Eberhard, 1985; 2010a; b). By comparison, female genitalia

64   have been considered to be less diverse in shape (Eberhard, 1985), and have been much less

65   studied (Ah-King *et al.*, 2014). However, recent studies using more quantitatively rigorous

66   approaches that focus on overall shape rather than traditional linear measurements, have

67   demonstrated the large amount of variation in female genital shape (Brennan & Prum, 2012;

68   2015; Showalter *et al.*, 2014; Orbach *et al.*, 2018). Studies of genital variation are key to

69   disentangling evolutionary hypotheses such as lock and key (Defour, 1844; Tanabe & Sota,

70   2008; Wojcieszek & Simmons, 2012; 2013), female choice (Bonet *et al.*, 2013), and sexually

71   antagonistic evolution (Arnqvist & Rowe, 2002; Brennan & Prum, 2012).

72   Discerning the coevolutionary processes that shape female and male genital morphology

73   could better our understanding of how morphological diversity in copulatory structures arises

74   and persists (Brennan, 2016). In addition, vaginal shape data can help inform the potential

75   influence of reproductive processes associated with pregnancy, parturition, and/or oviposition

76   (Brennan, 2016), but these ideas have rarely been tested. Since the 1990s, geometric

77   morphometrics (GM) has revolutionized the study of comparative morphology and shape

78   evolution (Bookstein, 1991; Rohlf & Marcus, 1993) with the majority of this work being done on

79   hard tissue such as skulls (e.g., Zelditch *et al.*, 2008; Hedrick & Dumont, 2018) or postcranial

80   bones (e.g., Vander Linden *et al.*, 2018). However, since genitalia are made up of soft tissue, GM

81   has been infrequently applied to comparative morphological analyses of genitalia (but see

82   Macagno *et al.*, 2011; Showalter *et al.*, 2014; Orbach *et al.*, 2018). While previous traditional

83   morphometric studies using linear estimates of size and shape have confirmed earlier non-

84   morphometric work suggesting that female genitalia are not highly variable in shape (Eberhard,

85   2006), several more recent GM studies performed on female genitalia have demonstrated salient

86   and substantial shape diversity within and between taxa (Macagno *et al.*, 2011; Showalter *et al.*,

87   2014; Orbach *et al.*, 2018). For example, Orbach *et al.* (2018) showed that ontogeny and

88   evolutionary allometry led to differences in cetacean vaginal shape with some taxa having short,

89   wide vaginas and others having long, thin vaginas using two-dimensional GM. Not surprisingly,

90   GM appears to give better insights into shape than linear measurements (Adams *et al.*, 2004).

91   Spiny dogfish (*Squalus acanthias*) are one of the best-known species of fish in terms of

92   reproductive ecology, evolution, and morphology (Gilbert & Heath, 1972; Pudney & Callard,

93   1984; Callard *et al.*, 2005; Hamlett *et al.*, 2005; Musick & Ellis, 2005; Pratt & Carrier, 2005) and

94   thus represent a rare opportunity for better understanding the effects of vaginal shape on

95   reproduction. In spite of the developmental and evolutionary work on *S. acanthias* reproduction,

96   particularly related to their viviparity, there have not yet been any studies on the shape of the

97   spiny dogfish vagina. Female *S. acanthias* have two oviducts, which run posteriorly along the

98   dorsal body wall and continue in a caudal direction, turning into vaginal tissue that continues to

99   the cloacal opening (Fishbeck & Sebastiani, 2015). The urinary papilla, through which urine is

100   excreted, is located in the middle of the cloaca, and slightly protrudes from the cloacal opening

101   (Fishbeck & Sebastiani, 2015). Like all elasmobranchs, spiny dogfish have internal fertilization,

102   so selection via copulation may be important in determining vaginal shape. Pregnancy can be a

103   major burden on female bodies, especially in *S. acanthias*, which has a 24-month gestation

104   period, one of the longest in living vertebrates (Ketchen, 1972; Nammack *et al.*, 1985; Jones &

105   Ugland, 2001; Natanson *et al.*, 2017). As such, the effects of pregnancy on genital morphology

106   could provide a window into the possible causes for high intraspecific genital variation found in

107   other vertebrates (Orbach *et al.*, 2018). Here, we examine the effect of pregnancy on vaginal

108   shape for the first time using geometric morphometric methods to broaden the understanding of

109   female genital morphological evolution.

110   We evaluate several questions pertaining to spiny dogfish reproduction but also the usage

111   of geometric morphometrics in the study of vaginal shape. Specifically we ask: (**1**) Are there

112   differences between the ontogenetic allometric trajectories of non-reproductive (e.g., fin size)

113   and reproductive traits (e.g., genital size)? If vaginal size is under sexual selection, we predict

114   that it will exhibit positive allometry with respect to body length, as a result of sexually selected

115   pressures at the onset of sexual maturity, while non-reproductive traits will have isometric trends.

116   (**2**) Does the vagina change shape due to pregnancy? We predict that specimens that are visibly

117   pregnant will have significantly different shapes from specimens that are not visibly pregnant as

118   the tissues stretch to allow parturition. We also predict larger vaginal asymmetry in specimens

119   that are pregnant given that females accommodate large embryos alternating in their uterus and

120   therefore one large embryo is always closer to the vaginal entrance on one side. (**3**) Does three-

121   dimensional geometric morphometrics (3DGM) reveal clearer trends than two-dimensional

122   geometric morphometrics (2DGM) when studying soft tissues? Since vaginas are three-

123   dimensional structures, we predict an increase in morphospace separation between pregnant and

124   non-pregnant specimens using 3DGM, but similar overall trends because the vaginal shape of

125   this species is relatively simple.

126

127   **Materials and Methods:**

128   **(a) Sample**

129   A commercial fisherman collected a sample of 22 female spiny dogfish (*Squalus*

130   *acanthias*) off of the coast of Rhode Island in August and September of 2017. These specimens

131   were collected under Federal Exempted Fishing Permit #17013. Each shark was measured for a

132   number of traits using traditional linear morphometrics including total body length, pectoral fin

133   width and length, vagina length, oviduct length, cloacal slit length, sperm gland length and width,

134   and tail fork length (Table S1). Further, the number of embryos in the uterus of each pregnant

135   shark was counted. Specimens were categorized into one of three reproductive states: visibly

136   pregnant (n = 10), not visibly pregnant, but reproductive (developed egg yolk present) (n = 10),

137   and not reproductive (n = 2). Visibly pregnant sharks were those females with visible embryos

138   developing anywhere in their oviduct. Early pregnancy can be difficult to detect so we refer to

139   reproductively mature females with no visible embryos in their oviducts as not visibly pregnant

140   rather than not pregnant. All sharks were near adulthood or were adults (body length = 77.9–94.9

141   cm–Ketchen, 1972). We considered fin related measurements to be selected for through natural

142   selection, given the primary purpose of the fin is for locomotion. Although female shark fins are

143   commonly grasped by male sharks during copulation, and may therefore be partially influenced

144   by sexual selection, we found no published evidence that fin biting has been observed in dogfish

145   sharks and found no bite marks on the female fins during our dissection. Gilbert and Heath

146   (1972) hypothesized that *Squalus* mating is similar to *Scyliorhinus calnigula*, where males coil

147   their flexible body around the female, rather than biting her fins.

148   Prior to dissection, 3D molds of the complete vaginal lumen were made using Elite HD+

149   Super Light Body dental silicone, following a similar technique used to cast vaginal lumen shape

150   in humans (Pendergrass *et al.*, 1996). 3D models were then generated through photogrammetry

151   using the 3DF Zephyr lite software (3Dflow SRL, Verona, Italy). Each silicone mold was

152   photographed on a rotating stool completely around its circumference, so that at least 70 photos

153   were obtained per mold for use in model reconstruction. We used a Canon EOS Rebel T5i,

154   camera with a 100 mm lens, mounted on a tripod and a set of four LED lights to obtain excellent

155   quality photos.

156   Following successful model creation, the vagina was dissected out, including the cloacal

157   slit and the posterior region of the oviducts. Specimens were then mounted on a template to

158   ensure consistent orientation in photographs and photographed using a Canon EOS Rebel T5i

159   camera such that each vagina filled the same percentage of the camera field of view (Zelditch *et*

160   *al.,* 2012).

161

162   **(b) Traditional morphometric analyses (Question 1)**

163   We evaluated allometric differences between naturally and sexually selected traits by

164   performing linear regression of our log-transformed measurements based on 21 dogfish sharks in

165   the basic *stats* package in R (R Core Team, 2017). To this end, we extracted allometries for our

166   naturally selected traits by regressing total length onto two pectoral fin measures (pectoral fin

167   width at the base of the fin, and fin length along the proximal and distal sides of the fin), and

168   extracting the slope value. Reproductive characters were also compared with total length

169   including vagina length, sperm gland width and length, cloacal slit length, and oviduct length.

170   Confidence intervals were calculated based on ordinary least squares regressions using the

171   confint function in the *stats* package in R to determine if variables were negatively allometric (m

172   < 1), isometric (m $= 1$), or positively allometric (m > 1). Given significant correlations with size

173   for some variables, residuals of each variable's relationship with total length were compared with

174   reproductive state. Only two sharks were non-reproductive in this sample so non-reproductive

175   sharks were pooled with non-visibly pregnant reproductive sharks for traditional morphometric

176   analyses.

177

178   **(c) Geometric morphometric analyses (Question 2 and 3)**

179   Two-dimensional landmarks (n = 12) and semi-landmarks (n = 7 curves, 55 semi-

180   landmarks) were digitized on photographs (Fig. 1A) in TPSDig2 (Rohlf, 2006) (see Table S2 for

181   a complete list of landmarks and landmark descriptions). All landmarks were taken by Patricia

182   Antalek-Schrag (PA) to eliminate inter-observer error. Each image was landmarked three

183   separate times to quantify intra-observer measurement error given the difficulty of landmark

184 placement in soft tissues (Lee, 1982; Carpenter, 1996, Arnqvist & Martensson, 1998; Orbach *et*

185 *al.*, 2018). Landmark data were then imported into R (R Core Team, 2017) and opened in the

186 *geomorph* package (Adams & Otárola-Castillo, 2013). Generalized Procrustes Analysis (GPA)

187 was performed translating, rescaling, and rotating the landmark configurations into the same

188 shape space (Zelditch *et al.,* 2012). Sliding semi-landmarks were slid by minimizing bending

189 energy between adjacent semi-landmarks (Perez *et al.,* 2006).

190   Given that vaginas are biologically asymmetric, we ran a multi-factor ANOVA with

191 individuals (symmetric variation), sides (directional asymmetry), and the interaction between

192 individuals and sides (fluctuating asymmetry) as factors (Klingenberg & McIntyre, 1998; Mardia

193 *et al.,* 2000). This allowed separation of the symmetric and asymmetric components of total

194 shape variation (Klingenberg & McIntyre, 1998). We then tested whether asymmetry in the

195 vagina made up a significant portion of total variation using the η^2 effect size metric (Olejnik &

196 Algina, 2003). To assess whether asymmetry was higher in not-visibly pregnant female vaginas

197 or visibly pregnant females, we re-ran these analyses separating out the not-visibly pregnant and

198 visibly pregnant specimens. These analyses parse out the relative contribution of each factor as a

199 percentage and were represented using a heatmap where hotter colors represent larger

200 contributions of a factor to total shape variation and cooler colors represent smaller contributions.

201   Prior to doing statistical analyses, we used an exploratory principal component analysis

202 (PCA) to evaluate differences in morphospace occupation between groups. The difference

203 between vagina shape and both reproductive state and number of embryos was statistically

204 examined by taking a consensus shape (mean) of all three replicates per specimen and then using

205 a Procrustes ANOVA at an alpha level of 0.05 (Goodall, 1991). Additionally, we examined the

206 relationship between only the symmetric component of total shape variation and both

207 reproductive state and the number of embryos in order to determine whether the asymmetric

208 component of variation was obscuring underlying signals. Finally, the common allometric

209 component (CAC) of shape data (Mitteroecker *et al.,* 2004; Drake & Klingenberg, 2008) was

210 compared to vaginal centroid size and shark total body length to evaluate the effects of body size

211 on the data. The CAC calculates shape scores based on a regression of shape against size, which

212 is the allometric trend in the data. A significant relationship between the CAC and size implies a

213 significant allometric trend.

214   To evaluate potential differences in our data between 2DGM analyses and 3DGM

215 analyses, we placed three-dimensional landmarks (n = 16 landmarks, 6 curves with 112 semi-

216 landmarks total) on 3D models (Fig. 1B, C) using Landmark Editor (Wiley *et al.,* 2005). As with

217 the 2D analysis, we repeated the landmark and curve placement three times for each specimen to

218 calculate 3D landmarking error. Note that 3D analyses include 22 specimens and 2D analyses

219 only include 18 specimens in exploratory analyses. Landmarks were converted into a tps format

220 using custom code written by Andrew J. Conith (AJC) and were then subjected to GPA with

221 semi-landmarks slid using the bending energy criterion. Analyses in 3D followed those

222 performed in 2D to allow for a comparison of data quality. Differences between the two datasets

223 were considered qualitatively using PCA as well as quantitatively using partial least squares

224 (PLS) analysis. The PLS analysis used the subset of the 3D specimens present in the 2D dataset

225 to allow for comparison. Note however that the landmark configurations for the 2D dataset and

226 3D dataset are not perfectly complementary. 2DGM requires that all landmarks be in a single

227 plane, a constraint not present in 3D data. Further, our 2D data were derived from images of the

228 vagina itself whereas 3D data were derived from internal molds of the vagina. As a result, we

229 opted to select landmark configurations that best represent the 2D and 3D shapes following a

230 previous study (Buser et al., 2018) to address our biological questions rather than imperfectly

231 select complementary landmarks.

232

233 **Results**

234 **(a) Traditional morphometric analyses**

235   Pectoral fin width was significantly correlated with body length ($p < 0.001$), scales with

236 positive allometry, and explained a substantial amount of variation ($R^2 = 0.51$) (Fig. 2; Table S3).

237 However, neither pectoral fin distal length ($p = 0.136$, $R^2 = 0.113$) nor pectoral fin proximal

238 length ($p = 0.819$, $R^2 = 0.002$) were significantly correlated with body length. When comparing

239 the relationship between residuals of fin measurements with reproductive status (not visibly

240 pregnant and visibly pregnant specimens), only pectoral fin proximal length was significant ($p =$

241 0.008) with non-visibly pregnant females having larger residuals than visibly pregnant females.

242   We found no significant correlations with regard to the relationship between traditional

243 morphometric measurements of reproductive characters (vagina length–$p = 0.657$, $R^2 = 0.011$,

244 sperm gland width–$p = 0.154$, $R^2 = 0.104$, sperm gland length–$p = 0.169$, $R^2 = 0.097$, and

245 oviduct length–p = 0.408, R^2 = 0.036) and body length (Fig. 3). Only cloacal slit length was

246 correlated with body length (p < 0.001, R^2 = 0.437), which scaled isometrically. Reproductive

247 characters did not significantly differ between not visibly pregnant and visibly pregnant

248 specimens based on residuals of body length (Fig. 3).

249

250 **(b) Geometric morphometric analyses**

251   A multi-factor ANOVA was performed in both 2D and 3D to better quantify vaginal

252 asymmetry (Table S4). In 2D, fluctuating asymmetry was significant (p < 0.001), but directional

253 asymmetry was not significant (p = 0.708) and neither was individual variation (p = 0.892).

254 Based on effect sizes, individual variation (symmetric component) comprised 52.3% of total

255 variation, directional asymmetry comprised 17.8%, fluctuating asymmetry comprised 27.3%, and

256 measurement error comprised 2.5%. Similarly, in 3D only fluctuating asymmetry was significant

257 (p < 0.001), but effect sizes were differently distributed. Individual variation comprised 44.2% of

258 total variation, directional asymmetry comprised 30.6%, fluctuating asymmetry comprised

259 23.4%, and measurement error comprised only 1.7%. This demonstrates substantially higher

260 fluctuating asymmetry in both 2D and 3D than is commonly found in osteological structures

261 (Zelditch *et al.,* 2008; Hedrick *et al.,* in press), but also low measurement error demonstrating

262 repeatability of the selected landmarks.

263   We ran Procrustes ANOVAs on both the means of all three replicates and on the

264 symmetric component of variation for both 2D and 3D analyses to test whether shape differed

265 between different reproductive categories (not reproductive, not visibly pregnant, but

266 reproductive, and visibly pregnant) and between different numbers of embryos in the oviduct

267 (Table S5). Neither the symmetric component nor the means data had significant correlations

268 with either reproductive state or number of embryos. We additionally tested the relationship

269 between means shape and both vaginal centroid size and total length as well as the symmetric

270 component of variation and vaginal centroid size and total length for both 2D and 3D analyses.

271 Only the 3D means shape and vaginal centroid size had a significant correlation (p = 0.022)

272 suggesting a limited impact of body size on these data.

273   To address the issue of potential increased asymmetry during pregnancy, we further ran

274 separate multi-factor ANOVAs splitting our 2D and 3D data into pregnant and not visibly

275 pregnant/non-reproductive subgroups. Our 2D dataset had 8 visibly pregnant specimens and 10

276   not visibly pregnant specimens whereas our 3D dataset had 9 visibly pregnant specimens and 13

277   not visibly pregnant specimens. In the 2D data, there were similar effect sizes for all variables

278   (individual variation, directional asymmetry, fluctuating asymmetry, and measurement error)

279   between pregnant and not visibly pregnant specimens (Table S6). These trends were also similar

280   to the not visibly pregnant 3D data. However, the visibly pregnant specimens in 3D

281   demonstrated significant directional asymmetry, which made up 48.6% of total variation (Fig. 5)

282   Finally, a PCA for the 2D data revealed minimal separation between groups (Fig. 4a,

283   Tables S7, S8). Principal component (PC) 1 characterized 24.8% of total variance and PC 2

284   characterized 22.5% of total variance. Non-reproductive specimens plotted on opposite ends of

285   the PC1 axis and there was substantial overlap between visibly pregnant and not visibly pregnant

286   reproductive specimens. In 2D, PC1 describes asymmetric variation in the vagina, with negative

287   values indicating that the right side of the vagina is wider than the left, and positive values

288   indicating that the left side is wider. PC2 describes variation in the aspect ratio of the vagina with

289   positive values indicating a more elongated vagina, and negative values a shorter, squatter vagina.

290   In comparison, the 3D PCA revealed that variation in PC1 indicated changes in the aspect ratio

291   of the vagina, with positive values having shorter and wider vaginas than negative values. PC2

292   described variation in both asymmetry and width with positive values showing wider right sides

293   of the vagina, but also a wider vagina overall compared to the negative values, where the left

294   side of the vagina was wider. The 3D data revealed tight clustering of visibly pregnant specimens

295   with non-reproductive specimens in the upper right quadrant of morphospace (Fig. 4b) where

296   visibly pregnant females had shorter, wider vaginas and the right side was wider overall than the

297   left. Not visibly pregnant specimens were more widely dispersed in morphospace. However, this

298   separation and clustering in the 3D morphospace was not significantly different. Although no

299   such separation could be inferred from visualization in the 2D data, the PLS analysis did reveal a

300   significant association between the 2D and 3D data with an r-PLS correlation coefficient of 0.82.

301

302   **Discussion**

303   **(a) Selection and allometric trends**

304   Natural selection and sexual selection operate simultaneously on numerous structures,

305   often antagonistically and genitalia are no exception (reviewed in Brennan and Prum, 2015).

306   However, most studies evaluating the role of natural selection in genital morphology have been

307   done on males, even though natural selection on pregnancy and parturition is likely to be an

308   important force in shaping vaginal morphology (Brennan & Prum, 2015). To address whether

309   spiny dogfish vaginal morphology evolves in response to sexual selection, we assessed whether

310   reproductive traits show positive allometry compared to non-reproductive traits (following

311   Eberhard et al 2009). Surprisingly we found no significant correlation between body size and the

312   size of most traits we measured (reproductive and non-reproductive). Only cloacal slit length and

313   fin width were positively correlated with respect to shark total length. Cloacal slit length scaled

314   isometrically, while fin width scaled positively.

315

316   **(b) Pregnancy and shape**

317   Pregnancy could change the dimensions of the vagina and other reproductive traits.

318   Therefore, we also assessed whether traits were correlated with reproductive state under the

319   hypothesis that visibly pregnant females would have different dimensions in reproductive organs

320   than not visibly pregnant females. However, there were no significant associations between

321   allometrically corrected residuals of linear reproductive organ measurements and reproductive

322   state. The reasoning behind the lack of significant associations may be due to the low variance in

323   shark ontogenetic stages in our study since the majority of our sharks were already adult. It may

324   alternatively be due to a reduced signal as a result of shape not being adequately captured by

325   simple linear measurements. Therefore, we re-assessed these potential associations using GM.

326   Similar to the traditional measurements, 2DGM data did not uncover significant

327   associations between vaginal shape and vagina centroid size, shark total length, reproductive

328   state, or the number of embryos present in the oviducts at the time of death. For the 3D analyses,

329   there was a significant association only between vaginal shape and vaginal centroid size ($R^2 =$

330   0.102). Further, PCA demonstrated that shape variance for both reproductive states is

331   exceptionally high intra-specifically with tall, narrow vaginas on one end of the axis and stout,

332   wide vaginas on the other end of the axis (Fig. 4). Therefore, there appears to be a substantial

333   amount of within species shape variation present in spiny dogfish vaginas, evidently not related

334   to pregnancy. We note that although not significantly different from not visibly pregnant sharks,

335   visibly pregnant sharks tend to have short, wide vaginas based on the 3D data (Fig. 4b).

336   This study supports previous studies that have found vaginas to have high shape variance

337   (Polihronakis, 2006; Showalter *et al.,* 2014; Orbach *et al.,* 2018), contra to other studies, that

338   have found females have relatively small vaginal morphological variance (Eberhard, 1985;

339   Evans *et al.,* 2011). Orbach *et al.* (2018) found that two cetacean species (*Tursiops truncatus*,

340   *Phocoena phocoena*), for which large intraspecific samples were collected, had vagina shapes

341   ranging broadly across cetacean vaginal morphospace that included over 25 species. These

342   intraspecific differences could be partly explained by ontogeny, since they found significant

343   ontogenetic variation in their sample. Unfortunately, only a few specimens were pregnant

344   (Orbach *et al.,* 2018) so statistical analysis by reproductive state was not possible.

345   Given the exceptionally large gestational time in spiny dogfish (Ketchen, 1972), it is

346   surprising that vaginal shape was not found to significantly differ between visibly pregnant and

347   not visibly pregnant sharks. Our use of morphometric analyses likely did not cloud these trends

348   since the same results were found for linear measurements, 2DGM, and 3DGM. We suggest a

349   number of possibilities as to why our predictions were not met. First, it is possible that many of

350   the not visibly pregnant sharks had been previously pregnant and given birth, which may have

351   modified the shape of their vaginas causing those sharks to cluster near the visibly pregnant

352   sharks in 3D morphospace, increasing vagina shape disparity in not visibly pregnant sharks

353   substantially (Fig. 4b). Parity changes some dimensions of the vagina in humans (Pendergrass *et*

354   *al*. 2000; Barnhart *et al*. 2006), although whether these changes start during pregnancy and

355   whether they are permanent is unknown. This process has not been described in any other

356   vertebrate. Second, vaginal shape may be primarily driven by sexual selection, sexual conflict,

357   copulation, coevolution with male genitalia, or other factors unrelated to pregnancy that have yet

358   to be studied. It is clear that vaginas have high shape variance and future studies should focus on

359   uncovering the causes of that shape variance. Finally, Showalter *et al.* (2014) found overlapping,

360   but distinct shapes for two related watersnake species and suggested that low sample sizes may

361   be an issue when using GM on soft-tissue structures. Unfortunately, unlike hard tissues, fresh

362   soft-tissue data are often difficult to generate at large sample sizes due to the opportunistic

363   manner in which they are collected. Larger sample sizes in the future may help to clarify the

364   trends reported here. Future studies on other vertebrates will help to clarify the effects of

365   pregnancy on vaginal shape beyond the spiny dogfish. Given that this is the first study to

366   quantitatively assess the effects of pregnancy on vaginal shape in any vertebrate, our trends can

367   only be considered preliminary. However, using this study as a starting point, there are many

368 directions for additional studies to go to allow for a better understanding of the evolution of
369 female genitalia.
370
371 **(c) Asymmetry in soft-tissue structures**
372   All structures have some degree of bilateral asymmetry, manifested as directional
373 asymmetry and fluctuating asymmetry (Mardia *et al.*, 2000; Klingenberg *et al.*, 2002; Leamy &
374 Klingenberg, 2005; Willmore *et al.*, 2005; Dongen, 2006). Fluctuating asymmetry in particular is
375 often used to estimate the degree of canalization, the ability of a population to generate the same
376 phenotype regardless of environmental factors, and developmental stability, the ability of a
377 population to buffer against developmental noise. Directional asymmetry occurs when the left
378 and right sides of a bilaterally symmetric structure differ, but always in the same direction (e.g.,
379 fiddler crab claws).
380   Magnitudes of asymmetry as measured in two dimensions were quite similar between not
381 visibly pregnant and visibly pregnant specimens (~45–48% of total variation–Fig. 5). However,
382 in three dimensions, the trends were quite different between not visibly pregnant and visibly
383 pregnant specimens. Not visibly pregnant specimens had a similar level of fluctuating
384 asymmetry to that of 2D analyses, but directional asymmetry was higher (36% in comparison
385 with 20–25%). Visibly pregnant specimens in 3D had a completely different pattern with 48.5%
386 of total variation being captured by directional asymmetry and only 12% of total variation being
387 captured by fluctuating asymmetry. Given that spiny dogfish oviducts are paired and that pups
388 are distributed asymmetrically in the oviducts, it was not unexpected to find high vaginal
389 asymmetry (ranging from 45–61 percent of total variation) relative to studies of hard tissue,
390 where asymmetry typically accounts for less than 15% of total variation (Hedrick *et al.*, in press).
391 Therefore, the high asymmetry in these vaginas is functional rather than developmental in nature.
392 It appears this difference is exaggerated when the sharks are far into their pregnancy such that
393 directional asymmetry swamps both within species individual variation and fluctuating
394 asymmetry when sharks are measured in three dimensions (Fig. 5). As above, the 3D data
395 demonstrates this trend clearer than 2D data.
396
397 **(d) 2D or not 2D: dimensionality in soft-tissue**

398   As of 2014, Cardini (2014) reported that more than half of geometric morphometric

399   studies are performed in two-dimensions in spite of the fact that two-dimensions are clearly just

400   an approximation for 3D structures (Roth, 1993). Very few studies have examined the

401   differences between trends in 2D and 3D data either quantitatively or qualitatively. Cardini

402   (2014) found that up to 20% of total variation in marmot mandibles related to using two-

403   dimensional data to approximate 3D structures. She then questioned the results of a previous 2D

404   study she had done with those same data which showed that interspecific differences in 2D

405   mandibular shape of marmots accounted for 13–36% of total shape variance (Cardini, 2009).

406   Given the similarities in levels of variance between interspecific variance and variance between

407   2D and 3D analyses, using 2D proxies for 3D structures for some types of data (e.g., skulls) may

408   cloud real trends, especially in intraspecific analyses. For example, Buser et al. (2018) found

409   trends supported by 3DGM were not supported by 2DGM in cottid fish, likely a result of the

410   two-dimensional data not adequately capturing variation along the z-axis. This issue is likely

411   compounded when dealing with images of deflated soft-tissue structures rather than 2D images

412   of hard tissues (e.g., skulls).

413   In our analyses, given the high degree of dimensionality of vaginas, we characterized 2D

414   and 3D shape using different, but similar landmark configurations, as recently done by Buser et

415   al. (2018). Unfortunately, this precluded our ability to formally test the difference between our

416   2D and 3D data (Cardini, 2014). Using PLS analysis, we found a high correlation between our

417   2D and 3D datasets suggesting congruence between the data (r-PLS = 0.82). Still, what

418   constitutes a "good" correlation is somewhat arbitrary (Cardini, 2014). Cardini (2014) found that

419   2D images could approximate 3D structures for some datasets, but not others and found a range

420   of correlations (using the RV coefficient–Robert and Escoufier, 1976) of 0.623–0.873. Therefore,

421   our correlation of 0.82 may suggest relatively strong congruence between our 2D and 3D data.

422   Overall trends when examining vaginal shape versus vaginal centroid size, total length,

423   reproductive state, and the number of embryos present in the vagina showed consistent trends for

424   both 2D and 3D data in terms of both significance as well as variance explained by each variable.

425   However, morphospace occupation showed a lack of clustering among all three reproductive

426   categories in 2D, while it showed tight clustering for visibly pregnant specimens and non-

427   reproductive specimens in 3D. Shape trends along PC1 and PC2 were also quite different for 2D

428   and 3D analyses, which would lead to very different conclusions based on exploratory PCA. This

429   is important given that much of the understanding of shape change in GM studies relies on trends

430   derived from PCA. This problem will likely be compounded when examining more complex

431   vaginas than the ones found in spiny dogfish.

432

433   **Conclusions**

434   By using a geometric morphometric approach, we uncovered substantial shape variation

435   in spiny dogfish vaginas in comparison to traditional morphometric measurements. We did not

436   find that pregnancy influenced genital shape variation despite a very long pregnancy in this

437   species, suggesting that perhaps sexual selection, sexual conflict, or parturition may explain the

438   variation we found. We additionally suggest that incorporating three-dimensional analyses as

439   well as asymmetry analyses in female genital shape studies will further aid biologists in

440   uncovering how female genital shape has evolved. As geometric morphometrics becomes more

441   commonly used to assess soft-tissues, we stress both the importance of measuring asymmetry as

442   well as the likely importance of using 3DGM when characterizing complex three-dimensional

443   shapes such as vaginas (Cardini, 2014).

444

454

455   **References**

456   Adams, D.C. & Otárola-Castillo, E. (2013). geomorph: an R package for the collection and

457   analysis of geometric morphometric shape data. *Methods in Ecology and Evolution* 4, 393–

458   399.

459   Adams, D.C., Rohlf, F.J. & Slice, D.E. (2004). Geometric morphometrics: ten years of progress

460   following the 'revolution'. *Italian Journal of Zoology* 71, 5–16.

461   Ah-King, M., Barron, A.B. & Herberstein, M.E. (2014). Genital evolution: why are females still

462   understudied. *PLoS ONE* 12, e10011851.

463   Arnqvist, G. & Mårtensson, T. (1998). Measurement error in geometric morphometrics:

464   empirical strategies to assess and reduce its impact on measures of shape. *Acta Zoologica*

465   *Academiae Scientiarum Hungaricae* 44, 73–96.

466   Arnqvist, G. & Rowe, L. (2002). Antagonistic coevolution between the sexes in a group of

467   insects. *Nature* 415, 787.

468   Barnhart, K. T., Izquierdo, A., Pretorius, E. S., Shera, D. M., Shabbout, M., & Shaunik, A.

469   (2006). Baseline dimensions of the human vagina. *Human Reproduction*, *21*(6), 1618–1622

470   Bonet, S., Casas, I., Holt, W.V. & Yeste, M. (2013). *Boar reproduction: fundamentals and new*

471   *biotechnological trends*. Berlin: Springer.

472   Bookstein, F.L. (1991). *Morphometric tools for landmark data: geometry and biology*. New

473   York: Cambridge University Press.

474   Brennan, P.L.R. (2016). Studying genital coevolution to understand intromittent organ

475   morphology. *Integrative and Comparative Biology* 56, 669–681.

476   Brennan, P.L.R., Birkhead, T.R., Zyskowski, K., van der Waag, J. & Prum, R.O. (2008).

477   Independent evolutionary reductions of the phallus in basal birds. *Journal of Avian Biology*

478   39, 487–492.

479   Brennan, P.L.R. & Prum, R.O. (2015). Mechanisms and evidence of genital coevolution: the

480   roles of natural selection, mate choice, and sexual conflict. In *Sexual Conflict*. Rice, W. &

481   Gavrilets, S. (Eds.). Cold Spring Harbor, NY: Cold Spring Harbor Laboratory Press.

482   Brennan, P.L.R. & Prum, R.O. (2012). The limits of sexual conflict in the narrow sense: new

483   insights from waterfowl biology. *Philosophical Transactions: Biological Sciences* 367,

484   2324–2338.

485   Brown, W.M., Price, M.E., Kang, J., Pound, N., Zhao, Y. & Yu, H. (2008). Fluctuating

486   asymmetry and preferences for sex-typical bodily characteristics. *PNAS* 105, 12938–12943.

487   Buser, T. J., Sidlauskas, B. L. & Summers, A. P. (2018). 2D or Not 2D? Testing the Utility of 2D

488   Vs. 3D Landmark Data in Geometric Morphometrics of the Sculpin Subfamily Oligocottinae

489   (Pisces; Cottoidea). *Anatomical Record* 301, 806–818. doi:10.1002/ar.23752

490 Callard, I.P., George, J.E. & Koob, T.J. (2005). Endochrine control of the female reproductive

491 tract. In *Reproductive Biology and Phylogeny of Chondrichthyes: Sharks, Batoids, and*

492 *Chimaeras*: 283–300. Hamlett, W.C. (Ed.). Enfield, NH: Science Publishers.

493 Cardini, A. (2014). Missing the third dimension in geometric morphometrics: how to assess if

494 2D images really are a good proxy for 3D structures? *Hystrix, the Italian Journal of*

495 *Mammalogy* 25, 73–81.

496 Cardini, A., Nagorsen, D., O'Higgins, P. & Polly, P.D. (2009). Detecting biological

497 distinctiveness using geometric morphometrics: an example case from the Vancouver Island

498 marmot. *Ethology, Ecology, and Evolution* 21, 209–223.

499 Carpenter, K.E. (1996). Morphometric pattern and feeding mode in emperor fishes (Lethrinidae,

500 Perciformes). In *Advances in Morphometrics*: 479–488. Marcus et al. (Ed.). New York:

501 NATO ASI Series A: Life Sciences Vol 284, Plenum Press.

502 Defour, L. (1844). Anatomie generale des Dipteres. *Ann Sci Nat* 1, 244–264.

503 Dongen, S.V. (2006). Fluctuating asymmetry and developmental instability in evolutionary

504 biology: past, present, and future. *European Society for Evolutionary Biology* 19, 1727–1743.

505 Drake, A.G. & Klingenberg, C.P. (2008). The pace of morphological change: historical

506 transformation of skull shape in St Bernard dogs. *Proceedings of the Royal Society: Biology* 275,

507 71–76.

508 Eberhard, W.G. (2010b). Rapid divergent evolution of genitalia: theory and data updated. In *The*

509 *evolution of primary sexual characters in animals*: 40–78. Oxford: Oxford University Press.

510 Eberhard, W.G. (2010a). Evolution of the genitalia: theories, evidence, and new directions.

511 *Genetica* 138, 5–18.

512 Eberhard, W.G. (2006). Sexually antagonistic coevolution in insects is associated with only

513 limited morphological diversity. *Journal of Evolutionary Biology* 19, 657–681.

514 Eberhard, W.G. (1985). *Sexual selection and animal genitalia*. Cambridge, MA: Harvard

515 University Press.

516 Eberhard, W., Rodriguez, R. L., & Polihronakis, M. (2009). Pitfalls in understanding the

517 functional significance of genital allometry. *Journal of Evolutionary Biology*, *22*, 435–445.

518 Endler, J.A. (1995). Multiple-trait coevolution and environmental gradients in guppies. *Trends in*

519 *Ecology and Evolution* 10, 22–29.

520 Evans, J.P., Gasparini, C., Holwell, G.I., Ramnarine, I.W., Pitcher, T.E. & Pilastro, A. (2011).

521   Intraspecific evidence from guppies for correlated patterns of male and female genital trait

522   diversification. *Proceedings of the Royal Society: B* 278, 2611–2620.

523 Fishbeck, D.W., & Sebastiani, A.M. (2015) Comparative Anatomy: Manual of Vertebrate

524   Dissection. Morton Publishing Company. 576 pp.

525 Gilbert, P.W. & Heath, G.W. (1972). The clasper-siphon sac mechanism in Squalus acanthias

526   and Mustelus canis. *Comparative Biochemistry and Physiology* 42A, 97–119.

527 Goodall, C.R. (1991). Procrustes methods in the statistical analysis of shape. *J. R. Stat. Soc. B.*

528   53, 285–339.

529 Hamlett, W.C., Kormanik, G., Storrie, M., Stevens, B. & Walker, T.I. (2005). Chondrichthyan

530   parity, lecithotrophy, and matrotrophy. In *Reproductive Biology and Phylogeny of*

531   *Chondrichthyes: Sharks, Batoids, and Chimaeras*: 393–434. Hamlett, W.C. (Ed.). Enfield,

532   NH: Science Publishers.

533 Hedrick, B.P. & Dumont, E.R. (2018). Putting the leaf-nosed bats in context: A geometric

534   morphometric analysis of three of the largest families of bats. *Journal of Mammalogy*.

535 Hedrick, B.P., Schachner, E.R., Rivera, G., Dodson, P. & Pierce, S.E. The Effects of Skeletal

536   Asymmetry on Interpreting Biological Variation in the Fossil Record. *Paleobiology*.

537 Hosken, D.J. & Stockley, P. (2004). Sexual selection and genital evolution. *Trends in Ecology*

538   *and Evolution* 19, 87–93.

539 Jones, T.S. & Ugland, K.I. (2001). Reproduction of female spiny dogfish, Squalus acanthias, in

540   the Oslofjord . *Fishery Bulletin* 99, 685–690.

541 Ketchen, K.S. (1972). Size at maturity, fecundity, and embryonic growth of the spiny dogfish

542   (Squalus acanthias) in British Columbia waters. *Journal of the Fisheries Board of Canada* 29,

543   1717–1723.

544 Klingenberg, C.P., Barluenga, M. & Meyer, A. (2002). Shape analysis of symmetric structures:

545   quantifying variation among individuals and asymmetry. *Evolution* 56, 1909–1920.

546 Klingenberg, C.P. & McIntyre, G.S. (1998). Geometric morphometrics of developmental

547   instability: analyzing patterns of fluctuating asymmetry with Procrustes methods. *Evolution*

548   52, 1363–1375.

549 Leamy, L.J. & Klingenberg, C.P. (2005). The genetics and evolution of fluctuating asymmetry.

550   *Annual Review of Ecology, Evolution, and Systematics* 36, 1–21.

551   Lee, J.C. (1990). Sources of extraneous variation in the study of meristic characters: the effects

552   of size and inter-observer variability. *Syst. Zool.* 39, 31–39.

553   Macagno, A.L.M., Pizzo, A., Parzer, H.F., Palestrini, C., Rolando, A. & Moczek, A.P. (2011).

554   Shape - but Not Size - Codivergence between Male and Female Copulatory Structures in

555   Onthophagus Beetles. *PLoS ONE* 6(12), e28893.

556   Mardia, K.V., Bookstein, F.L. & Moreton, I.J. (2000). Statistical assessment of bilateral

557   symmetry of shapes. *Biometrika* 87, 285–300.

558   Mitteroecker, P., Gunz, P., Bernhard, M., Schaefer, K. & Bookstein, F.L. (2004). Comparison of

559   cranial ontogenetic trajectories among great apes and humans. *Journal of Human Evolution*

560   46, 679–698.

561   Musick, J.A. & Ellis, J.K. (2005). Reproductive evolution of chondrichthyans. In *Reproductive*

562   *Biology and Phylogeny of Chondrichthyes: Sharks, Batoids, and Chimaeras*: 45–79. Hamlett,

563   W.C. (Ed.). Enfield, NH: Science Publishers.

564   Nammack, M.F., Musick, J.A. & Colvocoresses, J.A. (1985). Life history of spiny dogfish off

565   the northeastern United States. *Trans. Am. Fish. Soc.* 114, 367–376.

566   Natanson, L.J., McCandles, C.T., James, K. & J. Hoey. (2017). Gestation period and pupping

567   seasonality of female spiny dogfish (*Squalus acanthias*) off southern New England. *Fish.*

568   *Bull.* 115, 473–483.

569   Olejnik, S. & Algina, J. (2003). Generalized eta and omega squared statistics: measures of effect

570   size for some common research designs. *Psychological Methods* 8, 434–447.

571   Orbach, D.N., Hedrick, B.P., Würsig, B., Mesnick, S.L. & Brennan, P.L.R. (2018). The

572   evolution of genital shape variation in female cetaceans. *Evolution* 72, 261–273.

573   Pendergrass, P.B., Reeves, C.A., Belovicz, M.W., Molter, D.J. & White, J.H. (2000).

574   Comparison of vaginal shapes in Afro-American, Caucasian and Hispanic women as seen

575   with vinyl polysiloxane casting. *Gynecol Obst Inves* 50, 54–59.

576   Pendergrass, P. B., Reeves, C. A., Belovicz, M. W., Molter, D. J., & White, J. H. (1996). The

577   shape and dimensions of the human vagina as seen in three-dimensional vinyl polysiloxane

578   casts. *Gynecologic and obstetric investigation*, *42*(3), 178–182.

579   Perez, S.I., Bernal, V. & Gonzalez, P.N. (2006). Differences between sliding semi-landmark

580   methods in geometric morphometrics, with an application to human craniofacial and dental

581   variation. *Journal of Anatomy* 208, 769–784.

582 Polihronakis, M. (2006). Morphometric analysis of intraspecific shape variation in male and

583 female genitalia of Phyllophaga hirticula (Coleoptera: Scarabaeidae: Melolonthinae). *Annals*

584 *of the Entomological Society of America* 99, 144–150.

585 Pratt, H.L. & Carrier, J.C. (2005). Elasmobranch courtship and mating behavior. In *Reproductive*

586 *Biology and Phylogeny of Chondrichthyes: sharks, batoids and chimaeras*: 129–169. Hamlett,

587 W.C. (Ed.). Enfield, NH: Science Publishers.

588 Pudney, J. & Callard, G.V. (1984). Development of agranular reticulum in Sertoli cells of the

589 testis of the dogfish Squalus acanthias during spermatogenesis. *The Anatomical Record* 209,

590 311–321.

591 R Core Team. (2017). R: A language and environment for statistical computing. R   Foundation

592 for Statistical Computing, Vienna, Austria. URL   https://www.R-project.org/ accessed

593 November 2017. (accessed May 2017).

594 Rohlf, F.J. (2006). tpsDig, digitize landmarks and outlines, version 2.05. Department of Ecology

595 and Evolution, State University of New York, Stony Brook, New York.

596 Rohlf, F.J. & Marcus, L.F. (1993). A revolution in morphometrics. *TREE* 8, 129–132.

597 Roth, V. (1993). On three-dimensional morphometrics, and on the identification of landmark

598 points. In *Contributions to Morphometrics*: 41–61. Madrid: Museo Nacional de Ciencias

599 Naturales.

600 Showalter, I., Todd, B.D. & Brennan, P.L.R. (2014). Intraspecific and interspecific variation of

601 female genitalia in two species of watersnake. *Biological Journal of the Linnean Society* 111,

602 183–191.

603 Simmons, L.W. (2014). Sexual selection and genital evolution. *Austral Entomology* 53, 1–17.

604 Tanabe, T. & Sota, T. (2008). Complex copulatory behavior and the proximate effect of genital

605 and body size differences on mechanical reproductive isolation in the millipede genus

606 Parafontaria. *The American Naturalist* 171, 692–699.

607 Vander Linden, A., Hedrick, B.P., Kamilar, J.M. & Dumont, E.R. (2018). Atlas morphology,

608 scaling and locomotor behaviour in primates, rodents and relatives (Mammalia:

609 Euarchontoglires). *Zoological Journal of the Linnean Society*.

610 Wiley, D.F., Amenta, N., Alcantara, D.A., Ghosh, D., Kil, Y.J., Delson, E., Harcourt-Smith, W.,

611 Rohlf, F.J., St John, K. & Hamann, B. (2005). Evolutionary morphing. *Proceedings of IEEE*

612 *Visualization*, 431–438.

613   Willmore, K.E., Klingenberg, C.P. & Hallgrímsson, B. (2005). The relationship between

614   fluctuating asymmetry and environmental variance in rhesus macaque skulls. *Evolution* 59,

615   898–909.

616   Wojcieszek, J.M. & Simmons, L.W. (2013). Divergence in genital morphology may contribute

617   to mechanical reproductive isolation in a millipede. *Ecology and Evolution* 3, 334–343.

618   Wojcieszek, J.M. & Simmons, L.W. (2012). Evidence for stabilizing selection and slow

619   divergent evolution of male genitalia in a millipede (Antichiropus variabilis). *Evolution:*

620   *International Journal of Organic Evolution* 66, 1138–1153.

621   Zelditch, M.L., Wood, A.R., Bonett, R.M. & Swiderski, D.L. (2008). Modularity of the rodent

622   mandible: integrating bones, muscles, and teeth. *Evolution and Development* 10, 756–768.

623   Zelditch, M.L., Swiderski, D.L., Sheets, H.D. & Fink, W.L. (2012). *Geometric Morphometrics*

624   *for Biologists: A Primer*. 2 edn. London, UK: Elsevier Academic Press.

625

626

627   **Figures:**

628   **Figure 1** Landmark configurations for (a) 2D and (b, c) 3D shape analyses.

629

630   **Figure 2** Allometric relationships (left) and comparisons between pregnant and not visibly

631   pregnant sharks (right) for naturally selected fin characters. (a) pectoral fin width, (b) pectoral fin

632   distal length, and (c) pectoral fin proximal length. Triangles = not reproductive, circles = not

633   visibly pregnant, but reproductive (egg yolk present), pluses = visibly pregnant.

634

635   **Figure 3** Allometric relationships (left) and comparisons between pregnant and not visibly

636   pregnant sharks for reproductive characters (right). (a) vagina length, (b) sperm gland length, (c)

637   cloacal slit length, and (d) oviduct length. Triangles = not reproductive, circles = not visibly

638   pregnant, but reproductive (egg yolk present), pluses = visibly pregnant.

639

640   **Figure 4** Principal components analysis of (a) 2D geometric morphometric data and (b) 3D

641   geometric morphometric data with TPS grids and landmark configurations showing the major

642   shape changes occurring along principal components 1 and 2. Replicates of each individual

643   connected with black lines. Black squares = non-reproductive, red circles = not visibly pregnant,

644   but reproductive, blue triangles = visibly pregnant.

645

646   **Figure 5** Heatmap showing the relative contributions of individual variation (symmetric

647   variation), directional asymmetry (DA), fluctuating asymmetry (FA), and measurement error

648   (ME) to the total variation in 2D and 3D pregnant and not visibly pregnant/non-reproductive

649   datasets. Cooler colors relate to low contributions to total variation and hotter colors relate to

650   high contributions to total variation. Note that directional asymmetry is particularly high in the

651   pregnant sharks rendered in three dimensions. Measurement error is low ($< 3\%$ of total variation)

652   in all datasets.

653

654   **Table S1** Spiny dogfish specimens with associated traditional measurements (fin and genital) as

655   well as reproductive state (not reproductive, not visibly pregnant, visibly pregnant) and number

656   of embryos present at time of death.

657

658   **Table S2** Landmark definitions including landmark number (reference with in-text figure 1),

659   landmark type, and definitions for each landmark.

660

661   **Table S3** Allometric regressions between natural selected traits (fin measurements), sexually

662   selected traits (genital measurements), and total length. Residuals of trait measurements were

663   then tested for correlations with reproductive state.

664

665   **Table S4** Asymmetry analyses for both the 2D and 3D geometric morphometric data splitting

666   variation into individual variation (symmetric component of variation), directional asymmetry,

667   fluctuating asymmetry, and measurement error. Procrustes ANOVAs were then done on the

668   individual variation component (symmetric component) and both reproductive state and number

669   of embryos to determine if the biological asymmetry was clouding potential trends.

670

671   **Table S5** Procrustes ANOVAs between the mean of specimen shape (across three replicates) and

672   vagina centroid size, total shark length, reproductive state, and the number of embryos present at

673   time of death. This was done separately for both 2D ($n = 18$) and 3D ($n = 22$) shape data.

674

675 **Table S6** Asymmetry analyses splitting specimens into not visibly pregnant/ not reproductive

676 and visibly pregnant categories to evaluate potential differences in effect sizes of asymmetry.

677 This was done separately for both 2D (n = 18) and 3D (n = 22) shape data.

678

679 **Table S7** Principal component scores, centroid sizes, and total length for both raw 2D geometric

680 morphometric data and means data. Additionally, PCA summaries are reported for each analysis
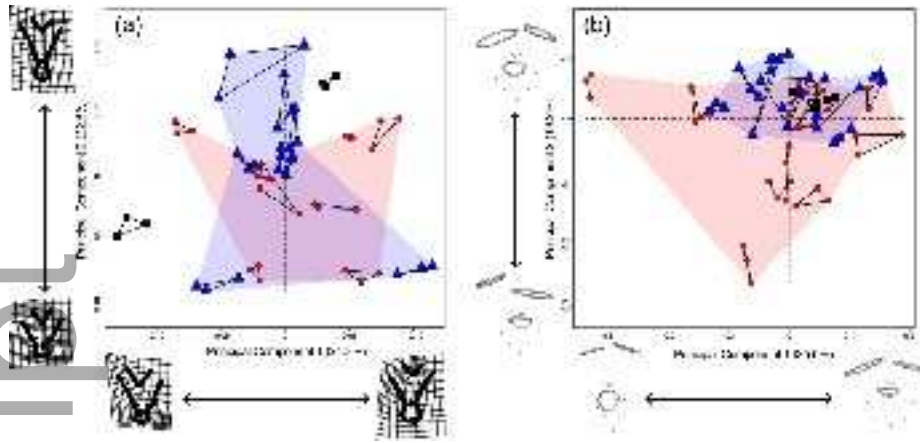
681 for the first 10 principal components.

682

683 **Table S8** Principal component scores, centroid sizes, and total length for both raw 3D geometric

684 morphometric data and means data. Additionally, PCA summaries are reported for each analysis

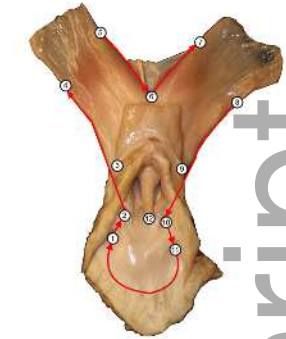685 for the first 10 principal components.
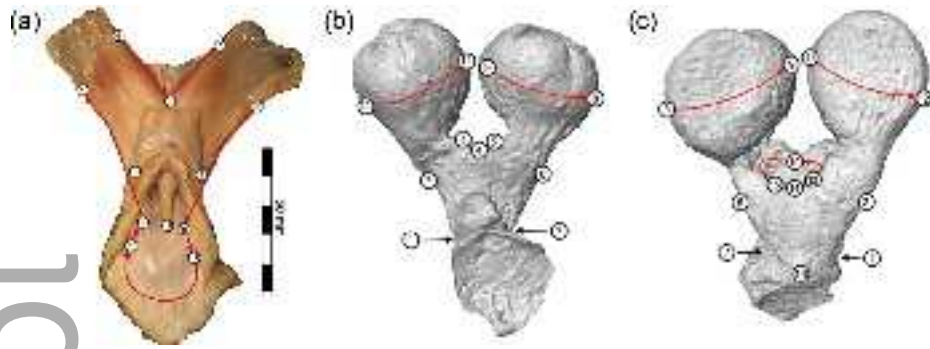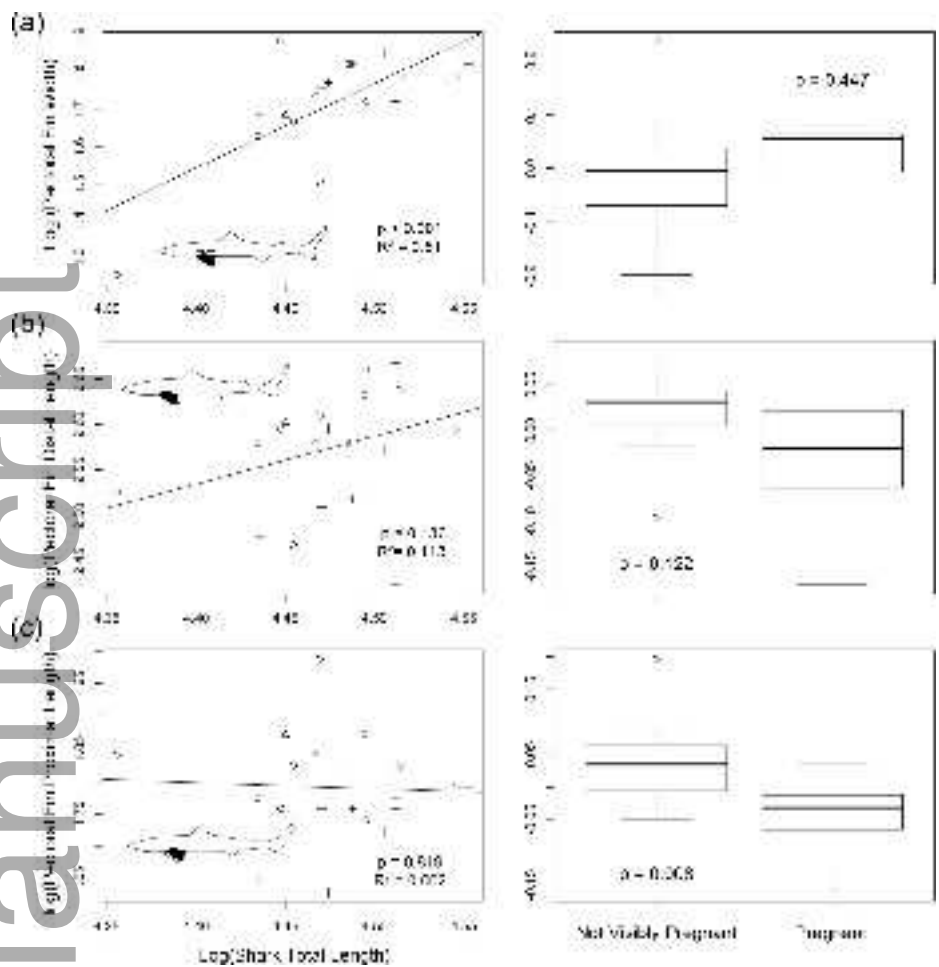
jzo_12653_f1.tif

jzo_12653_f2.tif
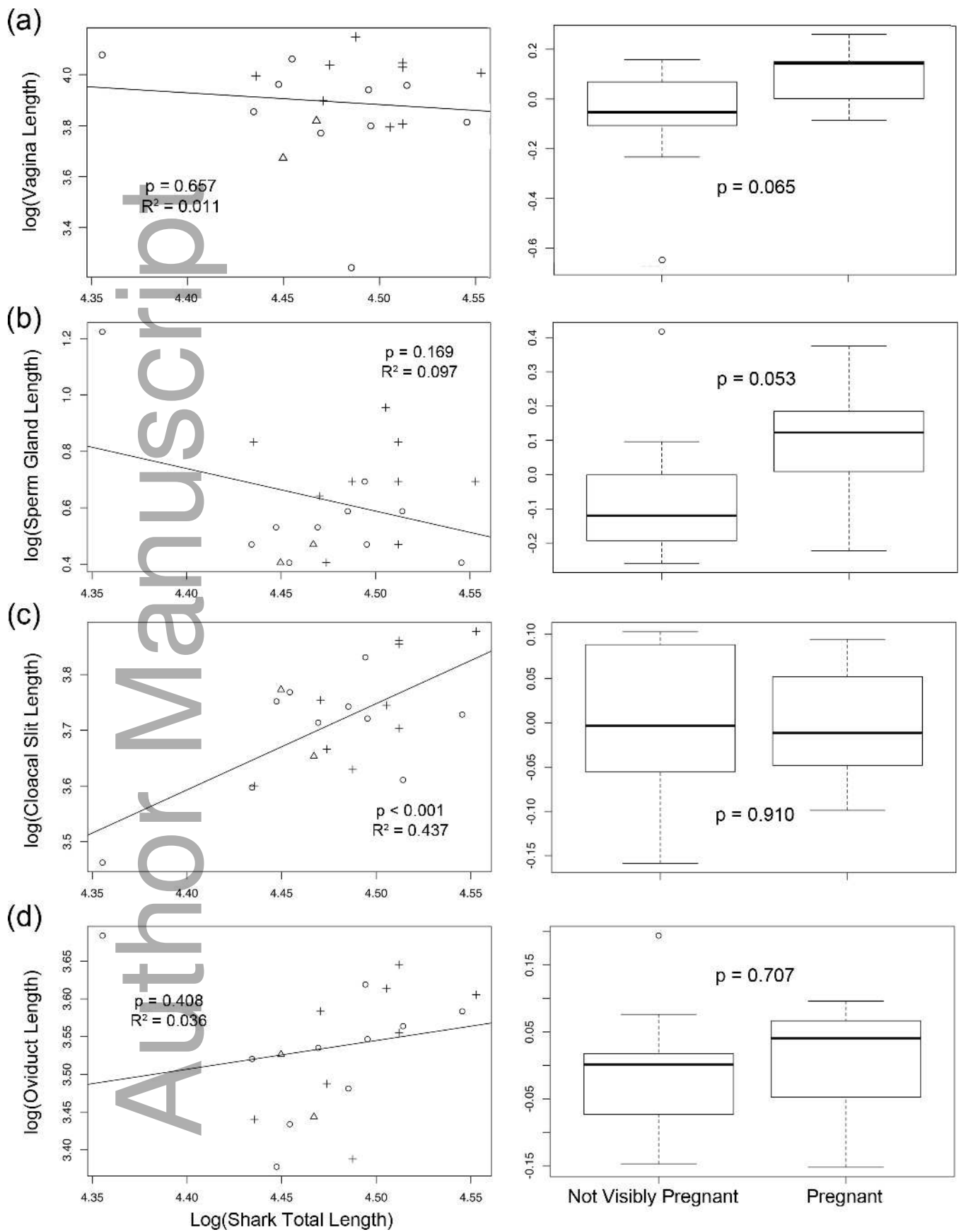
jzo_12653_f3.tif

jzo_12653_f4.tif

	Individual Variation	DA	FA	ME
Not visibly pregnant (2D)				
Pregnant (2D)				
Not visibly pregnant (3D)				
Pregnant (3D)				
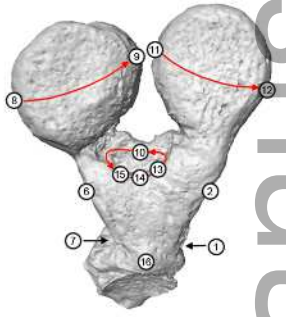
jzo_12653_f5.tif